FEBS Letters 429 (1998) 78–82 FEBS 20336

Structural stabilization of botulinum neurotoxins by tyrosine phosphorylation

José A. Encinar[a], Asia Fernández[a], José A. Ferragut[a], José M. González-Ros[a], Bibhuti R. DasGupta[b], Mauricio Montal[c], Antonio Ferrer-Montiel[c,*]

[a] *Department of Neurochemistry, University Miguel Hernández, C/Monóvar s/n (Polígono de Carrús), E-03206 Elche (Alicante), Spain*
[b] *University of Wisconsin, Madison, WI 53706, USA*
[c] *Department of Biology, University of California at San Diego, La Jolla, CA 92093-0366, USA*

Received 20 March 1998; revised version received 28 April 1998

Abstract Tyrosine phosphorylation of botulinum neurotoxins augments their proteolytic activity and thermal stability, suggesting a substantial modification of the global protein conformation. We used Fourier-transform infrared (FTIR) spectroscopy to study changes of secondary structure and thermostability of tyrosine phosphorylated botulinum neurotoxins A (BoNT A) and E (BoNT E). Changes in the conformationally-sensitive amide I band upon phosphorylation indicated an increase of the α-helical content with a concomitant decrease of less ordered structures such as turns and random coils, and without changes in β-sheet content. These changes in secondary structure were accompanied by an increase in the residual amide II absorbance band remaining upon H-D exchange, consistent with a tighter packing of the phosphorylated proteins. FTIR and differential scanning calorimetry (DSC) analyses of the denaturation process show that phosphorylated neurotoxins denature at temperatures higher than those required by non-phosphorylated species. These findings indicate that tyrosine phosphorylation induced a transition to higher order and that the more compact structure presumably imparts to the phosphorylated neurotoxins the higher catalytic activity and thermostability.

© 1998 Federation of European Biochemical Societies.

Key words: Protein structure; Protein folding; Metalloprotease; Fourier transform infrared; Exocytosis

1. Introduction

Botulinum neurotoxin (BoNT), considered the most potent neurotoxin and the sole cause of the neuroparalytic disease botulism, blocks acetylcholine release at the neuromuscular junction and thus produces flaccid paralysis in skeletal muscles [1,2]. Because of the extremely selective mode of action, inhibition of neurotransmitter release, BoNT is now an important therapeutic agent in the treatment of several neurological disorders associated with uncontrolled muscular contractions or spasms [3].

BoNT (serotypes A–G) is produced by the bacterium *Clostridium botulinum* as a single chain of 150 kDa which undergoes proteolytic cleavage yielding a fully active dichain protein composed of a 100-kDa heavy chain (HC) and a 50-kDa light chain (LC), linked by a disulfide bond. The neurotoxin first binds to a specific neuronal surface receptor, is internalized by receptor-mediated endocytosis, and the LC is then translocated to the cytosol, where it acts [1,4]. The LCs are Zn^{2+}-dependent metalloproteases that selectively cleave proteins involved in targeting and fusion of presynaptic vesicles with the plasma membrane [1,4–6]. The result is induction of nerve dysfunction by inhibiting Ca^{2+}-evoked neurotransmitter release.

The long lasting paralytic effects exerted by BoNT in botulism or in its therapeutic application suggest that these proteins are highly stable inside neurons at 37°C. This stability contrasts with the in vitro thermolability of pure BoNT implying structural difference(s) between the in vivo and in vitro forms [7,8]. Our discovery that tyrosine phosphorylation of BoNTs increases both their catalytic activity and thermal stability [7], suggests that significant changes in protein conformation may ensue, as reported for the phosphorylation of other proteins [9]. We examined this question by FTIR spectroscopy to monitor structural changes produced by phosphorylation of two neurotoxin serotypes, BoNT A and BoNT E, and differential scanning calorimetry to investigate the effect on their thermal denaturation process. Tyrosine phosphorylation of BoNT A and E increased their α-helix content, as evidenced from the conformationally-sensitive amide I bands [10]. The increment in structural order was accompanied by an increase in the absorbance of the amide II band remaining upon H-D exchange, suggesting that the phosphorylated neurotoxins are structurally more compact and less accessible to the solvent than the non-phosphorylated forms. Furthermore, the phosphorylation-induced structural change promoted a stabilization of the folded proteins that was reflected in an increase in the temperature at which the phosphorylated neurotoxins denature.

2. Materials and methods

Deuterium oxide (D_2O, 99.9% by atom) was purchased from Sigma. Centrifugal filter device Biomax-50K was from Millipore, Bedford, MA, USA. Recombinant Src kinase (specific activity 900 000 U/mg) was from Upstate Biotechnology, Lake Placid, NY, USA.

2.1. Phosphorylation of BoNT A and E

BoNT A and E were purified and tyrosine phosphorylated as described [7,11,12]. Briefly, 1 mg of neurotoxins in 500 μl of 20 mM HEPES (pH 7.4), 20 mM $MgCl_2$, 1 mM EGTA, 2 mM dithiothreitol, 0.5 mM ATP were incubated with 30 units of Src kinase for 90 min at 30°C. Non-phosphorylated and phosphorylated neurotoxins were kept at −80°C until used. Non-phosphorylated neurotoxin refers to samples in which ATP was omitted. Tyrosine phosphorylation was monitored by Western immunoblotting using a anti-phosphotyrosine monoclonal antibody (clone 4G10, UBI) as described [7]. To quantify tyrosine phosphorylation as mol Pi/mol neurotoxin a 40-μl aliquot of the phosphorylation reaction was supplemented with 5 μCi of [γ-^{32}P]ATP (3000 Ci/mmol). Phosphorylated neurotoxins were bound to phosphocellulose filters (SpinZyme, Pierce) and washed with 0.75%

*Corresponding author. Fax: (34) 6) 665 86 80.
E-mail: aferrer@umh.es

0014-5793/98/$19.00 © 1998 Federation of European Biochemical Societies. All rights reserved.
PII S0014-5793(98)00571-7

phosphoric acid. Phosphocellulose filters were immersed and equilibrated in scintillation fluid and the radioactivity was counted.

2.2. Infrared spectroscopy

BoNTs aqueous buffer was exchanged for deuterated buffer by subjecting the samples to two centrifugation cycles in a Biomax-50K filter, followed by incubation in D_2O-based buffer (10 mM HEPES buffer, pH 7.0, 130 mM KCl, 30 mM NaCl) for 2 h at ~20°C and, thereafter, another round of centrifugation cycles. Each sample of BoNTs (20 μl, at 8 mg/ml) was placed between a pair of CaF_2 windows separated by a 50-μm thick mylar spacer in a Harrick Ossining demountable cell. Spectra were recorded on a Nicolet 520 instrument equipped with a DTGS detector and the sample chamber was continuously purged with dry air. A minimum of 600 scans per sample were taken, averaged, apodized with a Happ-Genzel function and Fourier-transformed to give a nominal resolution of 2 cm^{-1} [13]. Three spectra at 20°C of each BoNT sample were recorded. Temperature was kept constant with a circulating water bath. Contribution of buffer spectra was subtracted and the resulting spectra used for analysis.

2.3. Determination of secondary structure components

Protein secondary structure components were quantified from curve-fitting analysis by band decomposition of the original amide I band after spectra smoothing [14,15]. Spectrum smoothing was carried out applying the maximum entropy method, assuming that noise and bandshape follow a normal distribution [14]. The minimum bandwidth was set to 12 cm^{-1} [14]. The resulting spectra possess a signal/noise ratio better than 4500:1. Derivation of IR spectra was performed using a power of 3, breakpoint of 0.3, and Fourier self-deconvolution was performed using a Lorenztian bandwidth of 18 cm^{-1} and a resolution enhancement factor (k) of 2.0 [16,17]. To quantify the secondary structure, the number and position of the absorbance band components were taken from the deconvoluted spectra, the bandwidth was estimated from the derived spectra, and the absorbance height from the original spectra [14]. The iterative curve-fitting process was performed in CURVEFIT running under SpectraCalc (Galactic Industries Corp., Salem, NH, USA). The number, position and bandshape were kept fixed during the first 200 iterations. The fittings were further refined by allowing the band positions to vary for 50 additional iterations. The goodness of fit between experimental and theoretical spectra was assessed from the χ^2 values (1×10^{-5}–4.5×10^{-5}). The area of the fitted absorbance band components was used to calculate the percent of secondary structure [13–18].

2.4. Differential scanning calorimetry

Differential scanning calorimetry (DSC) was performed on a Microcal MC-2 microcalorimeter, as described [19]. The difference in the heat capacities between 1-ml aliquots of BoNTs at 1 mg/ml (contained in the 'sample' cell of the instrument) and buffer alone ('reference' cell) were recorded by raising the temperature at a constant rate of 90°C/h.

3. Results and discussion

3.1. The helical content of BoNTs increases upon phosphorylation

The conformationally-sensitive amide I infrared absorbance band of BoNT A and E after tyrosine-specific phosphorylation (~0.5 mol Pi/mol toxin) were compared with non-phosphorylated neurotoxins. At this phosphorylation stoichiometry, both the LC and HC are similarly phosphorylated, and the activity and stability of the neurotoxins is augmented [7]. The original and the deconvoluted spectra of control and phosphorylated BoNTs samples are shown in Fig. 1. Tyrosine phosphorylation of BoNT A and E notably affected the spectral shape of the amide I band (Fig. 1, dashed lines). Although phosphorylated neurotoxins show the maxima observed in non-phosphorylated samples, the relative intensities of specific bands appear altered, suggesting that tyrosine phosphorylation modulates the relative content of secondary structural components. The individual components may be discerned upon application of resolution-enhancement and band-narrowing techniques [14,15]. Band-narrowing deconvolution of the amide I band showed that BoNT A and BoNT E exhibit maxima at approximately 1690, 1680, 1668, 1652, 1640, 1630 and 1615 cm^{-1}. Whereas the 1615-cm^{-1} component corresponds to amino acid side chain vibration, all the other maxima are assigned to vibration of the carbonyl group in peptide bonds within different secondary structural motifs [10]. The 1630-cm^{-1} component is assigned to β-structure, the 1640-cm^{-1} component to random structure, the 1652-cm^{-1} component to α-helix, the 1690- and 1668-cm^{-1} components to turns, and the 1680-cm^{-1} band includes contributions from

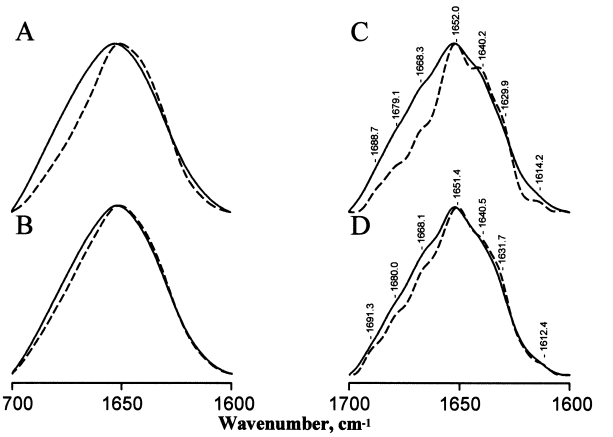

Fig. 1. Tyrosine phosphorylation modulates the secondary structure content of BoNT A and E. Infrared amide I band region of the original (A,B) and deconvoluted spectra (C,D) of BoNTA (A,C) and BoNT E (B,D) from control (solid line) and tyrosine phosphorylated samples (dashed line). Neurotoxins (8 mg/ml) were in D_2O medium prepared from 10 mM HEPES, pH 7.0, 130 mM KCl and 30 mM NaCl. Spectra were taken at 20°C and corrected from the buffer contribution by subtracting the spectrum characteristic of the buffer. Three spectra were acquired for each BoNT sample. Fourier self-deconvolution was carried out with a Lorentzian band of 18 cm^{-1} half-width, and a resolution enhancement factor of 2.0.

Table 1
Denaturation temperatures of non-phosphorylated and phosphorylated BoNTs

	BoNT A		BoNT E	
	Control	Phosphorylated	Control	Phosphorylated
T_d (°C) DSC[a]	51.1	53.0	50.5	53.2
T_d (°C) FT-IR[b]	50.5	53.5	51.3	55.1

[a]Denaturation temperatures were obtained from the DSC thermograms as the temperature at which the transition endotherm peaks [27,28]. Because of the need of large amounts of protein for DSC analysis, measures correspond to a single experiment.
[b]Denaturation temperatures correspond to the inflexion point of the sigmoidal curve obtained when the changes in the width at half-height of the amide I absorbance band are plotted as a function of the temperature (Fig. 4). Values correspond to three independent measurements. Experimental error is ≤ 10%.

turns as well as from the (0,π) β-sheet vibration band [10,20–22]. The secondary structures of non-phosphorylated and phosphorylated BoNTs were quantified using a maximum entropy method that reduces spectral noise providing a more accurate estimate of secondary structure [14,15]. Fig. 2 illustrates band-fitting analysis of the original amide I band of non-phosphorylated BoNT A (Fig. 2A) and BoNT E (Fig. 2B) and the corresponding phosphorylated species (Fig. 2C,D). Note that BoNT A shows a higher content of α-helix than BoNT E (Fig. 2E), consistent with other reports [23]. Upon phosphorylation, the α-helix content of BoNT A increased from 36% to 50% (Fig. 2E), and for BoNT E it augmented from 26% to 43% (Fig. 2E). This increment in α-helical structure was concomitant with a ≈40% decrease in less ordered structures such as turns (1668 cm^{-1}) and/or random coils (1640 cm^{-1}), without altering the β-sheet content (Fig. 2E). Therefore, these findings indicate that tyrosine phosphorylation promotes a disorder-to-order transition in the neurotoxin structure.

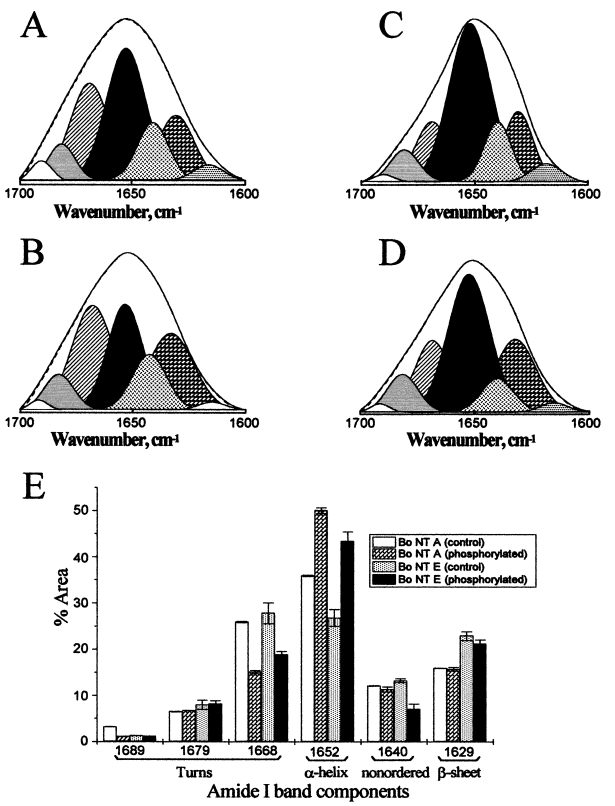

Fig. 2. Tyrosine phosphorylation increases the percent of α-helix secondary structure. Band-fitting analysis of the infrared amide I band of BoNT A (A,C) and BoNT E (B,D) from control (A,B) and phosphorylated samples (C,D). Each panel shows representative results from band-fitting analysis of BoNTs secondary structure. The discontinuous trace, superimposed on the original spectra, denotes the theoretical curve resulting from the contribution of all individual components, which are displayed as gaussian distributions under the spectra. E: Calculated percentages of all different components of the secondary structure of control and tyrosine phosphorylated BoNT A and BoNT E. Secondary structure elements were calculated by band decomposition and curve-fitting of the original amide I band after spectra smoothing [14,15]. Other conditions were as in legend to Fig. 1.

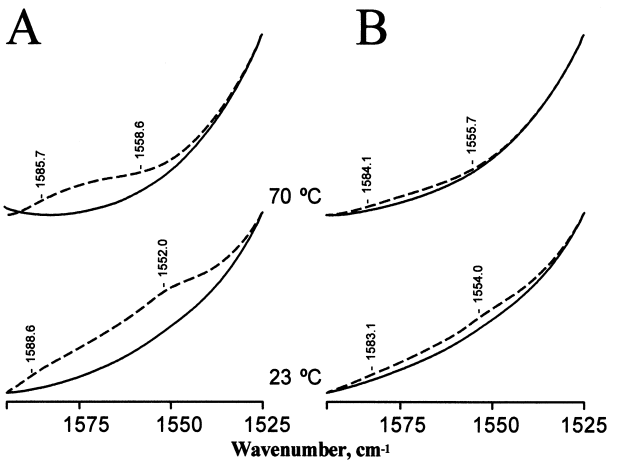

Fig. 3. Tyrosine phosphorylation of BoNT A and E promotes tighter packing. Phosphorylation-dependent changes in the amide II (1595–1525 cm^{-1} region) band of BoNT A (A) and BoNT E (B) remaining upon H-D exchange. Solid lines denote non-phosphorylated samples, and dashed lines indicate tyrosine-phosphorylated proteins. H-D exchange was carried out by 2-h incubation of samples in D_2O-based buffer followed by two washes with Biomax-50K centrifugal filters. The IR spectra were recorded in D_2O medium at the indicated temperatures during a heating cycle of 2.5 h. Protein concentration was 8 mg/ml. Contribution of buffer spectrum was subtracted.

3.2. The compactness of the BoNTs increases upon phosphorylation

The amide II band in proteins originates primarily from N-H bending in the peptide backbone [24,25]. Its residual intensity remaining after D_2O exchange arises from those NH groups unable to undergo H-D exchange and, therefore, it reports on the inaccessibility of the protein core to the solvent which, in turn, indicates the compactness of the protein [24,25]. Replacement of H_2O by D_2O from the non-phosphorylated neurotoxin resulted in the virtual disappearance of the amide II absorbance band centered at 1550 cm^{-1} (Fig. 3, lower panels, solid lines). Phosphorylated species, however, exhibited a substantial residual amide II band absorbance (Fig. 3, lower panels, dashed lines), which partly remained even after heating at 70°C (Fig. 3, upper panels). These results indicate a hindrance of H-D exchange in phosphorylated BoNTs, presumably because of the increased compactness of the structure. Taken together, the spectral changes in the amide I and the amide II upon phosphorylation suggest that the non-exchangeable hydrogens correspond to those involved in the newly generated α-helical structure.

3.3. The thermal stability of BoNTs increases upon phosphorylation

Non-phosphorylated neurotoxins displayed minor alterations on the spectral shape of the amide I band upon increasing the temperature up to 70°C (Fig. 4, solid lines). In contrast, for tyrosine-phosphorylated BoNTs the appearance of two components at 1618 and 1685 cm^{-1} (Fig. 4, dashed lines), which correspond to interactions between extended chains, was detected. This observation has been interpreted as a consequence of aggregation of thermally unfolded proteins [13,25–27]. The heat-induced denaturation process was irreversible as evidenced by the lack of recovery of the initial

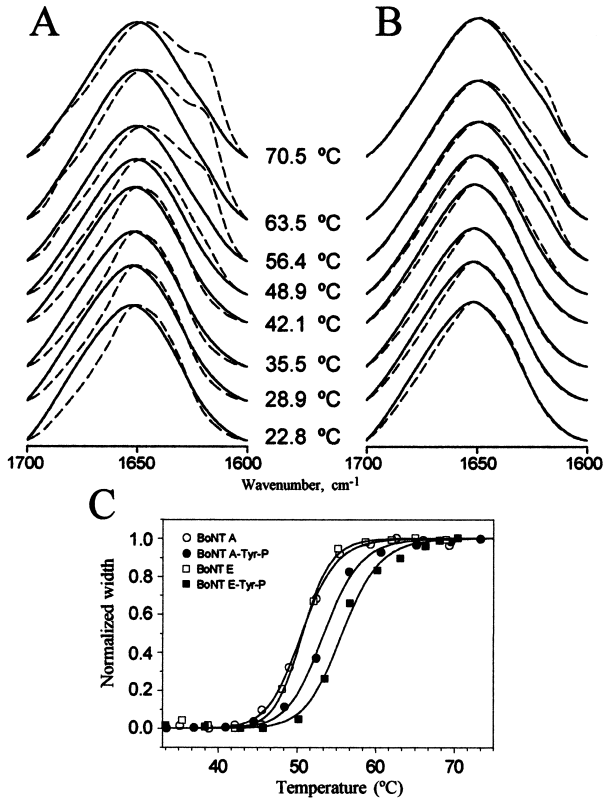

Fig. 4. Tyrosine phosphorylation increases the thermostability of BoNT A and BoNT E. Temperature dependence of the amide I band of BoNT A (A) and BoNT E (B) for control (solid line) and phosphorylated (dashed line) proteins. IR spectra were recorded in D_2O medium at the indicated temperatures during a heating cycle of 2.5 h. C: To determine the denaturing temperature, changes in the width at half-height of the amide I band were measured, normalized and plotted as a function of the temperature at which the spectrum was recorded. The data were described by the logistic equation:

$$\frac{w}{w_{max}} = \frac{1}{1+\left(\frac{T}{T_d}\right)^n}$$

where w denotes the width at half-height of the amide I band, w_{max} the maximal width at half-height, n the slope of the sigmoid, T the temperature, and T_d the denaturing temperature which corresponds to the inflexion point of the sigmoidal curve. Experimental data were fitted to the logistic equation with a non-linear least-squares regression algorithm using MicroCal ORIGIN version 2.8 (Microcal, Amherst). Solid lines depict the best fit to a sigmoidal curve. Denaturing temperatures are listed in Table 1.

spectral shape upon cooling the heated samples back to 20°C (data not shown).

The temperature-dependent changes in the width at half-height of the amide I IR band, plotted as a function of the temperature, display a sigmoidal shape with an inflexion point that corresponds to the denaturation temperature (Fig. 4C) [27]. Accordingly, BoNT A was found to denaturate at 50.5°C and BoNT E at 51.1°C, while phosphorylated BoNT A denatured at 53.5°C, and BoNT E at 55.1°C, i.e. 3–5°C higher than non-phosphorylated neurotoxins (Fig. 4C). The increased thermal stability was also detected by DSC, which measures directly the energetics of the heat-induced denaturation [28]. DSC demonstrated that phosphorylation induced a thermal stabilization, which was manifested as an increase of 2–3°C of the melting temperature (Table 1). These findings indicate that tyrosine phosphorylation of botulinum neurotoxins induces a conformation characterized by higher thermostability.

3.4. Structural basis of the functional modulation of BoNTs by tyrosine phosphorylation

Our findings show that tyrosine phosphorylation induces a disorder-to-order structural transition characterized by a significant increase in α-helical content with a decrease in less ordered structures. Consequently, phosphorylated BoNTs exhibit tighter packing than the non-phosphorylated species and denature at temperatures higher than those required for non-phosphorylated neurotoxins. The induction of structural order favors side chain interactions by hydrogen bond formation, an enthalpic gain. Higher order also augments the compactness of the protein, which presumably decreases the number of cavities, an entropic gain [9,29]. This mechanism to increase protein stability resembles that proposed to account for the extreme stability of thermophile enzymes, which are highly ordered and tightly packed structures [30]. We suggest that the more compact structure may account for the augmentation of the LC catalytic activity produced by tyrosine phosphorylation [7]. However, we cannot exclude a contribution of the HC to the structural changes observed in this study. Hence, additional studies are needed to determine the structural modulation of each neurotoxin chain by tyrosine phosphorylation.

Acknowledgements: This work was supported by grants from the Spanish DGICYT 95PM-0108 to (J.M.G.-R.) and PB93-0934 (to J.A.F.), the DAMD 17-93-C-3100 from the US Army Medical Research and Material Command (to M.M.), and an unrestricted generous gift from Athena Neurosciences (to B.R.D.G.). J.A.E. is recipient of a predoctoral fellowship from the Ministerio de Educación y Ciencia of Spain.

References

[1] Montecucco, C. and Schiavo, G. (1994) Molec. Microbiol. 13, 1–8.
[2] Ahnert-Hilger, G. and Bigalke, H. (1995) Prog. Neurobiol. 46, 83–96.
[3] Jankovic, J. and Hallett, M. (Eds.) (1994) Therapy with Botulinum Toxin, Marcel Dekker, New York, NY.
[4] Montecucco, C., Papini, E. and Schiavo, G. (1994) FEBS Lett. 346, 92–98.
[5] Jahn, R. and Südhof, T.C. (1994) Annu. Rev. Neurosci. 17, 219–246.
[6] Südhof, T.C. (1995) Nature 375, 645–653.
[7] Ferrer-Montiel, A.-V., Canaves, J.M., DasGupta, B.R., Wilson, M.C. and Montal, M. (1996) J. Biol. Chem. 271, 18322–18325.
[8] Kitamura, M., Sakaguchi, S. and Sakaguchi, G. (1969) J. Bacteriol. 98, 1173–1178.
[9] Johnson, L.N. and Barford, D. (1993) Annu. Rev. Biophys. Biomol. Struct. 22, 199–232.
[10] Braiman, M.S. and Rothschild, K.J. (1988) Annu. Rev. Biophys. Biophys. Chem. 17, 541–570.
[11] Sathyamoorthy, V. and DasGupta, B.R. (1985) J. Biol. Chem. 260, 10461–10466.
[12] Ferrer-Montiel, A.V., Montal, M.S., Díaz-Muñoz, M. and Montal, M. (1991) Proc. Natl. Acad. Sci. USA 88, 6418–6422.
[13] Fernández-Ballester, G., Castresana, J., Arrondo, J.L.R., Ferragut, J.A. and González-Ros, J.M. (1992) Biochem. J. 288, 421–426.
[14] Echabe, I., Encinar, J.A. and Arrondo, J.L.R. (1997) Biospectroscopy 3, 469–475.

[15] Bañuelos, S., Arrondo, J.L.R., Goñi, F.M. and Pifat, G. (1995) J. Biol. Chem. 270, 9192–9196.
[16] Moffatt, D.J., Kaupinnen, J.K., Cameron, D.G., Mantsch, H.H. and Jones, R.N. (1986) Computer Programs for Infrared Spectroscopy, NHCC Bulletin 18, National Research Council of Canada, Ottawa.
[17] Moffat, D.J. and Mantsch, H.H. (1992) Methods Enzymol. 210, 192–200.
[18] Surewicz, W.K., Mantsch, H.H. and Chapman, D. (1993) Biochemistry 32, 389–394.
[19] Artigues, A., Villar, M.T., Ferragut, J.A. and González-Ros, J.M. (1987) Arch. Biochem. Biophys. 258, 33–41.
[20] Arrondo, J.L.R., Mantsch, H.H., Mullner, N., Pikula, S. and Martonosi, A. (1987) J. Biol. Chem. 262, 9037–9043.
[21] Krimm, S. and Bandekar, J. (1986) Adv. Prot. Chem. 38, 181–364.
[22] Byler, D.M. and Susi, H. (1986) Biopolymers 25, 469–487.
[23] Singh, B.R., Wasacz, F.M., Strand, S., Jakobsen, R.J. and Das-Gupta, B.R. (1990) J. Protein Chem. 9, 705–713.
[24] Zhang, Y.P., Lewis, R.N.A.H., Hodges, R.S. and McEllaney, R.N. (1992) Biochemistry 31, 11572–11578.
[25] Baezinger, I.E. and Méthot, N. (1985) J. Biol. Chem. 270, 29129–29137.
[26] Surewicz, W.K., Leddy, J.J. and Mantsch, H.H. (1990) Biochemistry 29, 8106–8111.
[27] Castresana, J., Fernández-Ballester, G., Fernándes, A.M., Laynez, J.L., Arrondo, J.L.R., Ferragut, J.A. and González-Ros, J.M. (1992) FEBS Lett. 314, 171–175.
[28] Freire, E., Osdol, W.W., Mayorga, O.L. and Sanchez-Ruiz A, J.M. (1990) Annu. Rev. Biophys. Biophys. Chem. 19, 159–188.
[29] Shaw, A. and Bot, R. (1996) Curr. Opin. Struct. Biol. 6, 546–550.
[30] Szilagyi, A. and Zavodszky, P. (1995) Protein Eng. 8, 779–789.